Applied Catalysis B: Environmental 123–124 (2012) 182–192

Contents lists available at SciVerse ScienceDirect

Applied Catalysis B: Environmental

journal homepage: www.elsevier.com/locate/apcatb

Aging of photocatalytic coatings under a water flow: Long run performance and TiO_2 nanoparticles release

Josune Olabarrieta[a], Saioa Zorita[a], Iratxe Peña[a], Nerea Rioja[a], Oihane Monzón[a], Pablo Benguria[a], Lorette Scifo[b,*]

[a] Tecnalia-Environment Unit, c/Geldo, Parque Tecnológico de Bizkaia, Edificio 700, 48160 Derio, Spain
[b] Tecnalia-France, Immeuble MIBI, 672 rue du Mas de Verchant, 34000 Montpellier, France

ARTICLE INFO

Article history:
Received 21 November 2011
Received in revised form 19 April 2012
Accepted 20 April 2012
Available online 27 April 2012

Keywords:
Photocatalytic coatings
TiO_2 nanoparticles
Aging
Emissions
Water flow

ABSTRACT

Although photocatalytic coatings may experience severe wearing in most of their application, little work has been done to investigate their aging in a comprehensive way. In this article, we present an original experimental protocol to simulate an accelerated aging of photocatalytic coatings under a water flow, and test it on two materials: a well-known commercial product, Pilkington Activ™, and an experimental coating. The influence of intrinsic properties of the coatings (chemical nature, thickness) as well as environmental parameters (water matrix, UV-light) is investigated while the consequences of aging are evaluated under three different endpoints, related either to the long run performance of photocatalytic coatings or their environmental impact: (i) loss of the photocatalytic activity, (ii) degradation of mechanical properties, and (iii) release of TiO_2 nanoparticles. It is observed that both photocatalytic coatings experienced a deactivation of their active sites upon prolonged immersion. The extent of deactivation varies depending on the coating, being around 20% for experimental coatings and 65% for Pilkington Activ™ but shows little dependency on water matrix or illumination. An alteration of mechanical properties is seen on experimental coatings, which was accompanied by TiO_2 emissions as high as 150.5 $\mu g\,L^{-1}$. Although no reduction in film hardness or adhesion could be evidenced for Pilkington Activ™, TiO_2 concentrations up to 30.8 $\mu g\,L^{-1}$ was detected in the aging water showing that some release of TiO_2 nanoparticles also took place on this material. Interestingly, a common mechanism of release, triggered by an interaction between TiO_2, NaCl and UVA could be identified. Most severe damages were observed in presence of sodium chloride. These results suggest that the use of photocatalytic coatings with surface-bound nanoparticles in environmental applications may entail new entries of nanomaterials into the aqueous medium. They also prove that aging assays are an effective way of assessing the emissions.

1. Introduction

The photocatalytic properties of titanium dioxide (TiO_2) have made it a highly attractive material for environmental remediation. Under UV excitation, hole–electron pairs are indeed created in this semiconductor and initiate a series of oxidative and reductive reactions that can be employed to degrade a wide range of organic [1–3] and inorganic [4–6] contaminants. This photocatalytic reaction was proven to work both in the liquid and the gas phase. As a consequence, a large field of applications has emerged for it in self-cleaning surfaces, air purification and water treatment.

Despite other semiconductors demonstrate similar photocatalytic properties, TiO_2 remains by far the most employed photocatalyst, due to its low cost, good chemical stability, high reactivity and innocuousness. Over the years, it appeared moreover that reducing particle size could enhance the photocatalytic yields [7–9] as a result of an increased surface area and a reduction of volume recombination. Even if this effect seems to be counterbalanced below a certain size by a blue shift in the optical absorption of TiO_2, and a higher density of surface recombination sites, optimal photocatalytic efficiencies were reported for particle size ranging between 6 and 40 nm [10–15]. As a consequence, the use of nanoparticulate or nanostructured TiO_2 has today become a standard. Yet, all the recent work on nanoscience and nanotechnology unveiled that the properties of a nanomaterial can be significantly changed with respect to its bulk. In particular, concerns have been raised regarding the potential toxicity of nanoparticles. Adverse effects of TiO_2 nanoparticles have been observed on rat lungs [16–18], fish organs [19,20] and algae [21,22]. Although the results

* Corresponding author. Tel.: +34 667 178 915; fax: +33 4 67 13 01 25.
E-mail addresses: josune.olabarrieta@tecnalia.com (J. Olabarrieta), saioa.zorita@tecnalia.com (S. Zorita), pablo.benguria@tecnalia.com (P. Benguria), lorette.scifo@tecnalia.com (L. Scifo).

0926-3373/$ – see front matter © 2012 Elsevier B.V. All rights reserved.
http://dx.doi.org/10.1016/j.apcatb.2012.04.027

vary considerably from one study to another, and some standardized protocols are still needed to assess more precisely the toxicity of nanomaterials, there are therefore some hints that in spite of the low toxicity of the bulk, TiO_2 nanoparticles may present a risk for human health and the environment. Safety aspects should then be taken into account in the development of new TiO_2-based decontamination solutions, so that future environmental issues can be avoided and the expansion of this promising technology will not be hampered.

In contrast to nano-TiO_2 aerosols or suspensions, photocatalytic coatings present the advantage of immobilizing the nanoparticles on a support and therefore limit their spreading in the environment. As immobilization was also required in most industrial applications, a considerable market has emerged for photocatalytic coatings. The reliable immobilization of TiO_2 on various substrates has been previously reported by several authors [23,24]. However the adhesion of the coating to the substrate is usually evaluated directly after preparation or after a few cycles of use, and thereby is only representative of relatively new materials. Conversely, photocatalytic coatings are likely to experience severe wearing in outdoor applications or in water treatment. Hence, it is critical to figure out how immobilized TiO_2 will endure aging and if it will keep bound to the substrate over time [25,26].

The emission of TiO_2 nanoparticles to the aquatic environment, under natural weathering of painted exterior facades was recently evidenced by Kaegi et al. [27,28], suggesting that a similar release may occur on photocatalytic coatings. Efforts should then be made to try and detect the propensity of these materials to release TiO_2, and avoid further entry of TiO_2 nanoparticles to the environment. In this sense, Hsu and Chein [29] elaborated an experimental setup to simulate the action of wind, light and human contact on TiO_2 films and could observe significant emissions of TiO_2 nanoparticles in air under mechanical rubbing. Besides, they highlighted that in addition to the nature of the coating and the substrate, environmental parameters such as UV-light could influence the amounts of material released. Some attempts were also made to evaluate the resistance of photocatalytic coatings to water, submitting them to prolonged immersion [30], water jet [31] or a water flow [32]. However, in spite of their interesting approach, these studies often considered aging as a side issue and did not address it as a whole. Most of the time they remained focused on photocatalytic efficiencies and underestimated the issue of nanoparticles release, relying on indirect observations or rough estimates to evaluate the loss of photocatalyst. Moreover they neglected the impacts of aging on other characteristics of the coatings and lacked a deeper investigation of long-term effects.

Here, we present a comprehensive analysis of the aging under a water flow of two intrinsically different photocatalytic coatings and its impact on their macroscopic and microscopic properties. An experimental setup was developed to simulate an accelerated aging of the samples and the influence of several environmentally relevant parameters such as UV-light, and naturally occurring compounds (humic acids, sodium chloride) was thoroughly investigated. For the first time, the adequacy of different measurements to detect TiO_2 losses is discussed. Finally a relationship between structural changes in the photocatalytic coatings and the alteration of their macroscopic properties is established.

2. Experimental

2.1. Materials

Two photocatalytic coatings were investigated. One was a commercial product, Pilkington Activ™ (PA), which had been suggested by Mills et al. [33] as a reference material for photocatalytic coatings. According to manufacturer data and previous reports [33,34], it consists in a 12–15 nm thick nanocrystalline film of anatase TiO_2. It is deposited by an Atmospheric Pressure Chemical Vapour Deposition (APCVD) process on a glass substrate heated to 615 °C. The second material was an experimental coating, synthesized at low temperature in an external company and deposited by dip-coating. It contained in average 50 wt.% of TiO_2 nanoparticles (80% anatase, 20% rutile) embedded in a siliceous matrix. Two batches of experimental coatings (EC) with different thicknesses were studied in this work. Thin films were about 600 nm (EC-0.6) while the thick ones range 1 μm (EC-1).

All the samples were provided free of charge by the manufacturers or their distributors. They were supported on glass substrates and were cut to 30 mm × 25 mm tiles for the purpose of the experiment, without any further preparation. Methylene blue was purchased from Merck (Darmstadt, Germany), sodium chloride, nitric acid and sulphuric acid from Panreac (Barcelona, Spain). Humic acids of natural origin (humic acid sodium salt, technical grade, with lot number STBB1688) were obtained from Sigma–Aldrich (Steinheim, Germany). Their mineral content is detailed in Fig. S1 (Supplementary content).

2.2. Aging procedure

An accelerated aging procedure was developed in which 1 L water was circulated parallel to the surface of the coatings at 3 L min^{-1} for a period varying from 1 to 4 weeks. As shown in Fig. 1, the samples were placed in a Teflon® flume designed specifically for this experiment and water was pumped on them from a reservoir, by an EHEIM compact 1000 centrifugal pump (Zooplus). The water coming out of the flume was recollected in the reservoir and

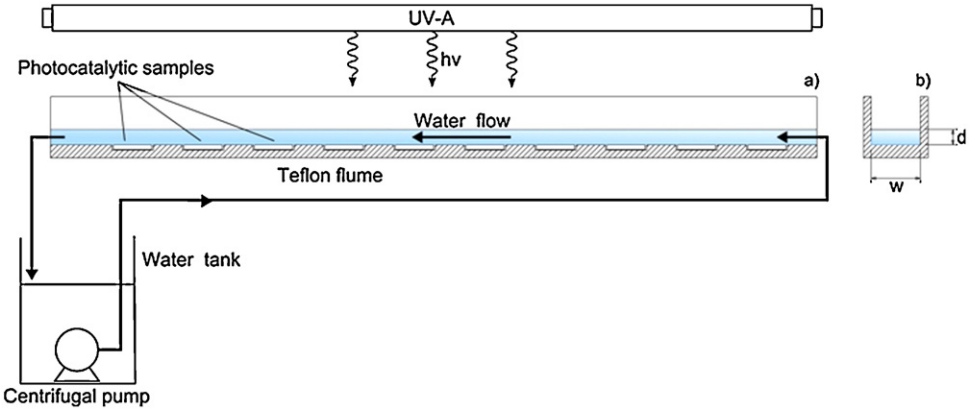

Fig. 1. Experimental aging setup: (a) longitudinal section and (b) cross-section.

Table 1
Composition of the water employed in the different aging experiments. In HA, NaCl and HA + NaCl runs, humics acids and sodium chloride were dissolved in deionized water to obtain the desired concentrations.

Run	[HA] (mg L^{-1})	[NaCl] (g L^{-1})
DW	0	0
HA	3	0
NaCl	0	10
HA + NaCl	3	10

re-circulated in the flume in a closed loop. Fresh water had to be added from time to time to compensate for evaporation.

The influence of natural compounds such as sodium chloride (NaCl) or humic acids (HA) on aging was investigated. As detailed in Table 1, four water matrixes (deionized water (DW), humic acids (HA), sodium chloride (NaCl) and humic acids plus sodium chloride (HA + NaCl)) were tested in order to evaluate the specific influence of each compound as well as their combined action. Pilkington Activ™ was aged under all water typologies. On experimental coatings however, a separation was made between the two batches, EC-0.6 samples being employed only in DW and HA runs while EC-1 samples were used for NaCl and HA + NaCl runs. All sample type/water combinations were probed in parallel in the dark and under UVA at *ca.* 1 mW cm^{-2}. For each experiment, the samples were divided into four groups depending on the time they were maintained in the flume: 1 week, 2 weeks, 3 weeks and 4 weeks. Each group comprised four replicates.

Based on experimental and water parameters, the Reynolds numbers of the flumes could be calculated in Table 2. Their values, slightly above 1000, places water flows at the onset of the turbulent regime. No pH or conductivity adjustments were performed. Their natural evolutions were monitored all over the experiments, as well as temperature (Fig. S2, Supplementary content). On average pH was found to be around 6 while temperature oscillated gently between 26 °C and 28 °C. Conductivity varied from one experiment to another but was generally raised over time, probably due to some dissolution phenomena.

2.3. Characterization of photocatalytic coatings

The photocatalytic activity of TiO_2 coatings was evaluated on all samples before and after aging, based on the degradation of methylene blue under UV-light, as described in normative JIS R 1703-2:2007. The samples were placed at the bottom of a 40 mm diameter cylindrical Pyrex cell filled with 35 mL 10^{-5} mol L^{-1} methylene blue solution. They were irradiated from the top by two F20T12 Hg 20 W Blacklight Blue fluorescent lamps purchased from GE lighting (Cleveland, OH, USA), which height was adjusted to ensure a radiation of 1 mW cm^{-2} at sample surface. The whole system was cooled by a fan. Every 20 min, a small volume of the reacting solution was extracted. Its absorbance at 664.7 nm was measured with a Jasco V-650 UV–vis spectrometer to determine the concentration in methylene blue.

The adhesion and hardness of the coatings were measured by the tape and pencil test methods, according to ASTM D 3359-08 and ASTM D 3363-05, respectively. In the tape test, a series of perpendicular cuts are made in the coating and a strip of tape is applied on this area. The adhesion grade (0B–5B) is determined by the percentage of coating removed, when pulling the tape off. For hardness measurements, a range of pencils with different hardness (6B <···< B <HB < F < H <···< 6H) are employed to draw short strokes at the surface of the coating. The hardness of the coating is defined by the minimum pencil hardness necessary to cut or gouge the film. In order to ensure a good positioning of the pencil and the application of a constant force, a Neurtek Instrument (Eibar, Spain) pencil hardness tester was used, resulting in a 2.9 N pressure. Given their destructive character, these two tests were only carried out once the samples aged. Control samples were used to determine initial hardness and adhesion.

The morphology and microstructure of the photocatalytic coatings were elucidated by Scanning Electronic Microscopy, with a Quanta 200 unit (FEI, USA) operated at an accelerating voltage of 25 kV. X-ray dispersive measurements (Adjustable EDAX Detecting Unit 132-10 for Quanta 200, FEI, USA) were performed to identify the different elements presents in the coatings, evaluate their spatial distribution and detect possible changes in the chemical composition of the coatings upon aging. An Atomic Force Microscope (Dimension TM 3100 SPM with Nanoscope III control unit, Digital Instruments, USA) was used in complement to observe fine structures, measure particles size, and determine the roughness of the coatings. Besides, and in order to evaluate possible changes in film thickness, sample surface was scratched with a cutter blade and the height of the resulting step was measured on AFM images. Silicon nitride cantilevers with a resonance frequency of 300 kHz were employed in the intermittent contact mode for all these measurements. The analysis of the data was performed with WSxM software [35] (Nanotec, Spain).

2.4. Loss of TiO_2

Very low levels of leaching were expected for both coatings and several complementary techniques were therefore applied with the intention of improving detection limits. First of all, the overall loss material was assessed, each sample being weighed before and after aging. Film thickness after aging was also measured by AFM and compared to that of a control sample, while variations in TiO_2 content were directly tracked through EDX measurements. The water circulated in each flume (1 L) was recollected at the end of the experiment and analyzed for TiO_2 with an axial Varian (Santa Clara, CA, USA) Vista-MPX CCD simultaneous ICP-OES, with SPS 5 sample preparation system. For each water, 2 × 80 mL were digested under gentle heating with 2 mL nitric acid 65% and 3 mL sulphuric acid 95% in order to dissolve TiO_2 nanoparticles before being injected. When extremely low amounts of TiO_2 were expected (DW and HA runs), 320 mL of the aging water were concentrated tenfold under a vacuum of 13 mbars at 40 °C and 1500 rpm using a Speed-Vac Concentrator (Savant SPD 131 DDA, Thermo Scientific, USA)

Table 2
Hydrodynamic parameters of the flumes.

Run	Q (m^3 s^{-1})	w (m)	d (m)	$R = wd/(w+2d)$ (m)	ρ (kg m^{-3})	μ (kg m^{-1} s^{-1})	$\nu = \mu/\rho$ (m^2 s^{-1})	$Re = QR/wd\nu$
DW					996.78 [63]	8.71×10^{-4} [63]	8.73×10^{-7}	1101
HA								
NaCl	5×10^{-5}	0.032	0.010	6.15×10^{-3}	1004.08 [64]	8.89×10^{-4} [64]	8.85×10^{-7}	1086
HA + NaCl								

Q, flow rate; w, flume width; d, water depth; R, hydraulic radius; ρ, solution density; μ, dynamic viscosity; ν, kinematic viscosity; Re, Reynolds number. Q, w and d are experimental parameters while ρ and μ were obtained from the literature [63,64]. Their values correspond to a temperature of 26 °C which is considered as the reference temperature in the flumes and a worst case scenario as it gives the lowest Reynolds numbers. Humic acids were found to have little influence on the solutions density and viscosity at such low concentrations, so that HA and HA + NaCl runs were considered equivalent to DW and NaCl, respectively.

before being digested and analyzed. The detection of Ti was made at 334.9 nm giving a detection limit of 0.16 $\mu g\,L^{-1}$ and a quantification limit of 0.52 $\mu g\,L^{-1}$. Each measurement was the average of four instrumental repetitions. Controls for each water typology were analyzed following the same procedure but no relevant levels of TiO_2 could be detected in them.

3. Results

3.1. Photocatalytic activity

The degradation rates obtained for methylene blue on experimental coatings and Pilkington Activ™, before and after aging, are presented in Fig. 2. A difference between the two coatings already arises from their initial photocatalytic activities. While the degradation rates achieved on experimental coatings range between 15% and 32%, the values obtained on Pilkington Activ™ keeps around 11%, probably due to the lower amount of TiO_2 it contains. Moreover two groups of samples can be distinguished among experimental coatings, corresponding to the two different batches. Indeed, if EC-0.6 samples (DW and HA runs) initially displayed a 30% degradation of methylene blue at 3 h, EC-1 samples (NaCl and HA + NaCl runs) hardly reached 15%. This result is surprising as thicker films generally have a better photocatalytic activity than thin ones, because of their higher photocatalyst load [36–38].

The evolution of the photocatalytic activity along the weeks of aging followed a very different pattern on the two coatings. For Pilkington Activ™, a loss of photocatalytic activity was detectable since the first week of aging, and the degradation rate kept decreasing continuously week after week. On the contrary, most samples of experimental coatings displayed an increase in their photocatalytic activity after the first week of treatment. A similar phenomenon was observed by Hidalgo and Bahnemann [39] for TiO_2 coatings prepared by thermal hydrolysis of $TiOSO_4$, which experienced a five times increment in their degradation rates after 150 h of continuous operation in a flow reactor. It was ascribed to the cleaning of the photocatalysts surface by the water flow and UV radiation. Although the increase in photocatalytic activity is much more moderate in our case (*ca* +10% for EC-0.6 and *ca* +90% for EC-1), a similar process is likely. As the measurement of the initial photocatalytic activity of the sample involves a 24 h exposure to UV light, it can be assumed that most of the cleaning process would take place before the beginning of the aging experiment. This would explain the lower extent of activity increase, the water flow only washing off last residues.

It is interesting to observe that the increase recorded for EC-0.6 and EC-1 coatings differs. Indeed if the improvement of photocatalytic activity is limited to a few percents on EC-0.6, degradation rates almost double for EC-1 samples. Also striking is the fact that the activity measured on EC-1 after 1 week of aging, perfectly matches the initial 30% degradation rates of EC-0.6, which is the value usually obtained on experimental coatings. A hypothesis is therefore that the low temperature synthesis of experimental coatings did not to enable a good structuring of thick EC-1 samples and that this process is completed during the first week of aging, through immersion in water. This seems besides to be confirmed by the higher thickness measured on EC-1 samples after aging (Table 3).

After this initial increase of photocatalytic activity, the degradation efficiencies of both batches of experimental coatings could generally be maintained to 30% until the second or third week of aging. They then experienced a slight decrease to finally stabilize around 25% after 4 weeks of aging. The degradation rates determined for Pilkington Activ™ at the same point are around 3–5%. A loss of photocatalytic properties therefore happens upon aging for both materials. Depending on the case, it varied from 27% to 78% on Pilkington Activ™. On EC-0.6 samples it accounted for about 20% of the initial activity, a similar value being obtained for EC-1 samples, if their improved degradation rates at 1 week of experiment are taken as a reference.

Among this panel, the results obtained on deionized water runs followed a rather divergent tendency. For both experimental and Activ™ coatings they display completely different behaviors depending on the illumination conditions, leading to the worst degradation rates but also their best values. A remarkable improve of the photocatalytic activity (+19.5%) is thus observed for EC-0.6 aged in deionized water and under dark conditions, while the same coating experienced a severe decrease in its degradation rate (−56.7% after 4 weeks) when aged under UVA. Besides the effect of UVA light on DW aging was opposite for the two coatings. It indeed entailed an important degradation of photocatalytic

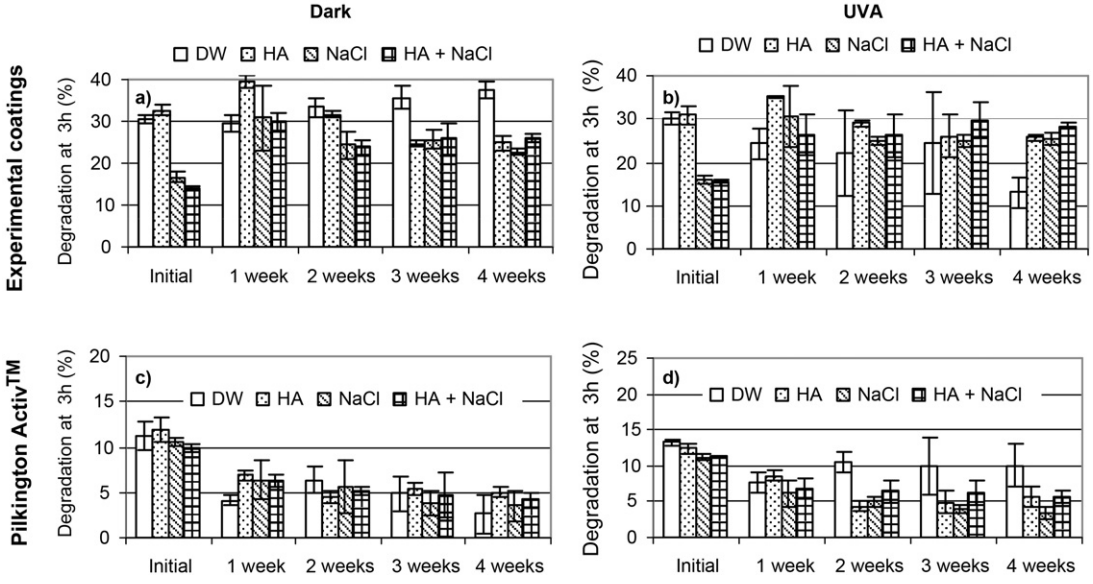

Fig. 2. Evolution of photocatalytic activity upon aging. Final degradation rates obtained by methylene blue test as a function of time for experimental coatings aged under (a) dark and (b) UVA and for Pilkington Activ™ glass, (c) dark and (d) UVA.

Table 3
Thickness and RMS roughness of control and aged samples as determined from AFM images. The thickness of Pilkington Activ™ coatings could not be measured correctly as the hardness of the samples made it impossible to scratch the coating without penetrating glass the substrate.

Sample	Coating	Water chemistry	Illumination	Thickness (nm)	RMS roughness
EC-control 1	EC-0.6	DW/HA	–	591.8 ± 31.8	45.7
EC-control 2	EC-1	NaCl/HA + NaCl	–	1033.3 ± 45.4	39.7
O10	EC-0.6	DW	Dark	583.0 ± 15.0	26.4
O25	EC-0.6	HA	Dark	571.9 ± 44.3	29.8
O42	EC-1	NaCl	Dark	1473.3 ± 18.5	24.9
O58	EC-1	HA + NaCl	Dark	1500.7 ± 33.5	19.6
L7	EC-0.6	DW	UVA	589.2 ± 41.9	29.7
L23	EC-0.6	HA	UVA	585.1 ± 2.4	44.6
L39	EC-1	NaCl	UVA	1663.3 ± 40.7	33.8
L55	EC-1	HA + NaCl	UVA	1231.0 ± 48.1	29.8
PA-control	PA	–	–		2.6
PO9	PA	DW	Dark	12–15 [33,34]	2.6
PO26	PA	HA	Dark		3.3
PO41	PA	NaCl	Dark		3.1
PO57	PA	HA + NaCl	Dark		3.7
PL8	PA	DW	UVA		2.3
PL24	PA	HA	UVA		5.5
PL40	PA	NaCl	UVA		3.6
PL56	PA	HA + NaCl	UVA		7.0

properties on EC-0.6 samples, while it mitigated the loss experienced by Pilkington Activ™ under dark conditions.

Apart from DW, the rest of the runs led to very similar results and an equivalent decrease of the degradation rate was observed after 4 weeks, on EC and Pilkington Activ™ respectively, for HA, NaCl and HA + NaCl runs. The presence or absence of UVA radiation in those runs did not seem to impact the photocatalytic properties of any of the coatings. Although humic acids were shown to induce a loss of photocatalytic activity it seems that the combination of both humic acid and NaCl did not result in further damages.

3.2. Mechanical properties

Pilkington Activ™ displayed at the same time a perfect adhesion to its glass substrate (5B grade on tape test scale) and a hardness above 6H, as is generally observed for photocatalytic coatings heated to high temperatures during their elaboration [40–42]. These properties could not be altered under the action of the water flow whatever the time of exposure, the water chemistry or the illumination condition. However it was suggested that mechanical response of very thin layers could be influenced for a great part by their substrate [43]. It is therefore possible that some mechanical degradation of the Activ™ coating remained undetected.

As can be seen in Fig. 3, the response of experimental coatings to mechanical testing was completely different. Although they demonstrated good mechanical properties at the beginning of the experiment, their adhesion to the substrate and hardness were strongly deteriorated by the aging process. As expected, thick films (EC-1 samples) proved to be the most fragile. Their initial mechanical properties were already lower than those of EC-0.6. Furthermore they record the strongest damages upon aging, even if this second

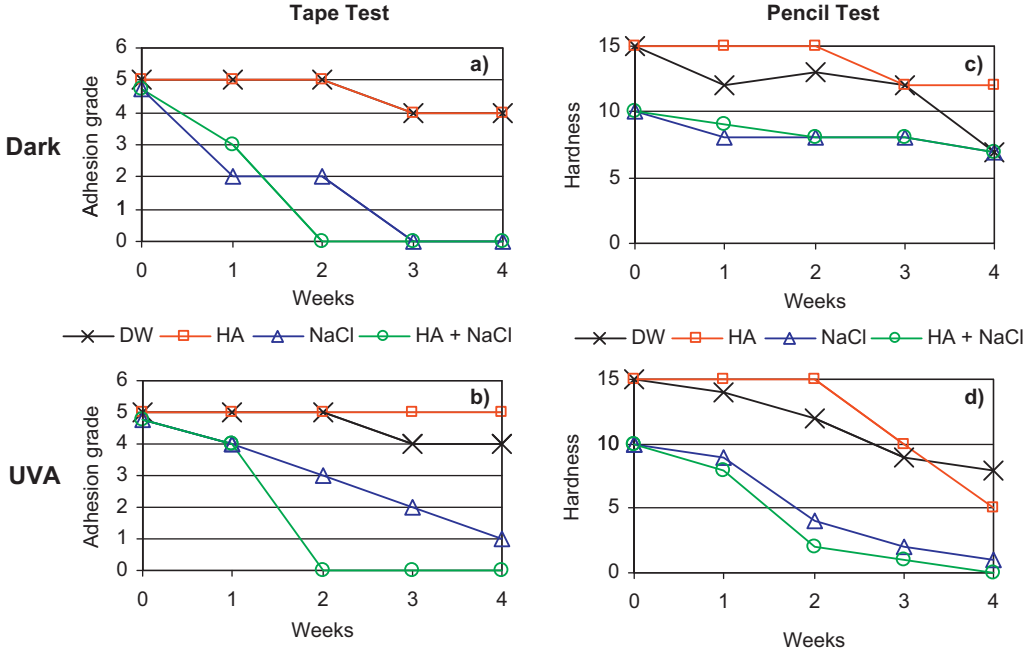

Fig. 3. Evolution of mechanical properties upon aging. Adhesion of EC-0.6 and EC-1 to the glass substrate based on the results of tape test after aging under (a) dark and (b) UVA radiation. (c) and (d) Hardness of the experimental coatings as evaluated by the pencil test. Standard graduations of pencil hardness going from 6B to 6H were converted to integer values from 1 to 14 for graphical representation. The values of 0 and 15 corresponded to hardness below 6B and above 6H, respectively.

point also has to be contrasted with the different aqueous matrix in which the two batches were aged.

A loss of adhesion is noticeable since the first week of experiment for EC-1 samples in NaCl runs, and after 3 weeks for DW and HA runs (EC-0.6 samples). Moreover the extent of deterioration also varied depending on water matrix and batch. A total loss of adhesion was achieved on EC-1 samples after 4 weeks of aging, while on EC-0.6 coatings the adhesion was only reduced to 4B and could even be maintained in HA run with UVA. On the whole, the magnitude of deterioration followed the sequence:

$$\underbrace{HA + NaCl > NaCl}_{EC\text{-}1} >> \underbrace{DW > HA}_{EC\text{-}0.6}$$

In spite of the initially lower mechanical properties of EC-1 samples it is therefore likely that the most relevant factor of degradation was the presence of 10 g L^{-1} sodium chloride in the aging water. Surprisingly, despite the fact that humic acids seemed to preserve the adhesion property better than deionized water alone on EC-0.6 samples, the aging process where humic acids and NaCl were combined on EC-1 samples proved to be the most aggressive. This suggests that some synergetic effect may occur between these two compounds, although a specific interaction between humic acids and EC-1 samples cannot be completely discarded.

Film hardness was also dramatically reduced over the aging process. Its decrease was immediate in all runs but HA, which resulted to be little aggressive and allowed maintaining high film hardness for 2 weeks. After 4 weeks of aging, the strongest deteriorations were observed for samples exposed to NaCl, with or without humic acids. This should anew be put into perspective with the initial lower hardness of EC-1 samples with respect EC-0.6.

It is striking that although HA, NaCl, and HA + NaCl runs all denoted a clear influence of UV-light on mechanical degradation, no difference in adhesion and hardness was observed between dark and UV samples in DW experiments. This shows that UV-light alone does not affect the coatings and neither does it damage them through photolysis. Its impact on the mechanical properties of experimental coatings must then be mediated through an interaction with humic acids or sodium chloride. Considering that adhesion was generally better maintained on UVA samples, we suggest that the radiation probably thwart the deteriorating effect of HA and NaCl on adhesion. An exactly opposite effect was observed for film hardness, where UVA induced the strongest deteriorations.

3.3. Morphology and microstructure

SEM images of a Pilkington Activ™ surface and an EC-1 sample are given in Fig. 4a and c. In spite of their different thicknesses, EC-0.6 and EC-1 samples had exactly the same morphology, and they will therefore be discussed jointly on the basis of Fig. 4c–e. At first sight both Pilkington Activ™ and experimental coatings display an apparently similar flat surface, where TiO_2 is homogeneously distributed, as can be seen on the EDX mapping of Ti element (Fig. 4b and d). However a closer look reveals several major differences between the two coatings. First of all, while the flatness of Pilkington Activ™'s surface is undisturbed, that of experimental coatings is punctuated with some protruding areas, which could be identified as TiO_2 in Fig. 4d. Upon magnification (Fig. 4e) these prominences disclose a granulated surface, which suggests they actually consist in an agglomeration of TiO_2 nanoparticles. In addition to TiO_2 agglomerates, the structure of the coating layer on EC samples seems to be significantly different from that of Pilkington Activ™. Indeed, the magnification of Fig. 4e hints to a mesoporous structure, which should favor the adsorption of the contaminants and their contact with the photocatalyst, contrary to the smooth surface displayed by Pilkington Activ™ whatever the magnification. A thorough examination of EDX data shows moreover a much higher density of TiO_2 on EC-0.6 and EC-1. This combined to the higher porosity of these films are most probably the reasons for the superior photocatalytic activity of experimental coatings over Pilkington Activ™.

To get a better idea of their fine structure the coatings were also imaged by Atomic Force Microscopy (Fig. 5). Due to their strong relief TiO_2 agglomerates could not be observed properly by AFM. The images shown here for experimental coatings only correspond to their background layer.

Despite the differences they exhibited on SEM images, both Pilkington Activ™ (Fig. 5a) and experimental coatings (Fig. 5b and c)

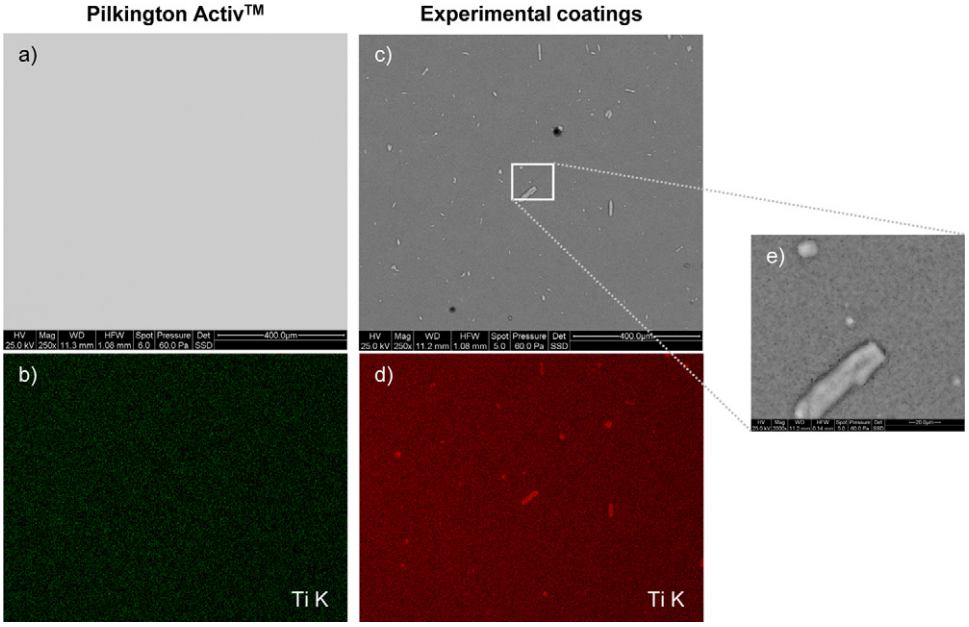

Fig. 4. Initial morphology of the two photocatalytic coatings. (a) SEM image of Pilkington Activ™ glass before aging and (b) corresponding elemental mapping. The green dots indicate the presence of Ti element. (c) SEM image of an EC-1 sample before aging and (d) corresponding elemental mapping. The red dots indicate the presence of Ti element. (e) Magnification of the area delimited by the white square in (c).

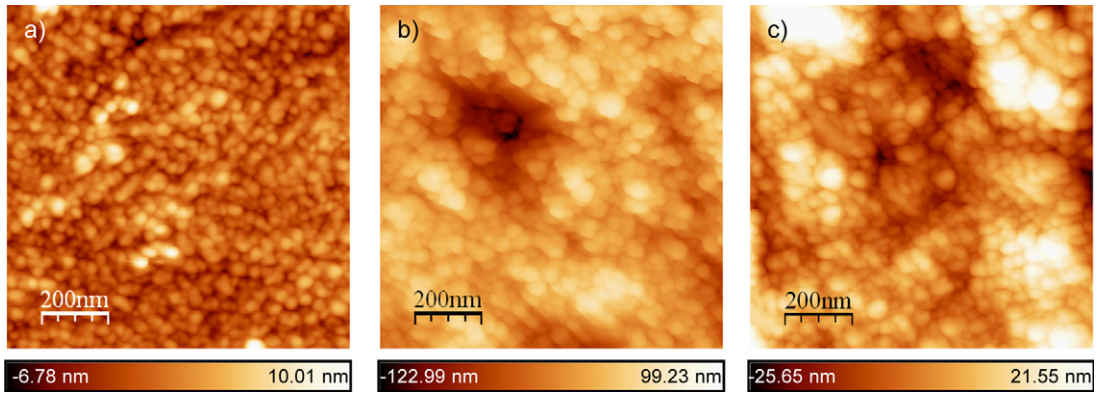

Fig. 5. Fine structure. AFM images (1 μm × 1 μm, 512 × 512 pixels) of the surface of (a) Pilkington Activ™, (b) EC-0.6 and (c) EC-1 acquired in the intermittent contact mode.

surface appear on AFM images as an aggregation of small particles. For Pilkington Activ™ a mean particle diameter of 40 ± 2 nm was found, which is slightly superior to the value of 30 nm measured by SEM by Mills et al. [33], but lower than the 95 nm reported by Chin and Ollis [34] based on their AFM images.

On experimental coatings, mean particle diameters of 48 ± 6 nm and 42 ± 4 nm were found for EC-0.6 and EC-1 respectively, which is also slightly higher than the size of the TiO_2 nanoparticles embedded in the coatings and therefore hints to a possible tip effect. The siliceous matrix could not be identified clearly. An initial RMS roughness of 45.7 nm (EC-0.6) and 39.7 nm (EC-1) (see Table 3) was measured for these coatings, which on the long range probably confers them their mesoporous aspect. The substantially lower value of 2.6 nm found for Pilkington Activ™ confirms for its part the flatness of this second type of coating.

No significant changes could be detected on AFM images after aging (not shown). The granular structure of the coatings was maintained and no clear tendency to a reorganization of TiO_2 nanoparticles could be evidenced. Neither the primary particles size, nor the surface coverage varied beyond the expected statistical fluctuations. However some deviation of the RMS roughness of aged samples with respect to their control values were noted (Table 3). The two coatings were affected in a very different way. Pilkington Activ™ glasses that were exposed to humic acids and UVA light, showed an enhanced roughness after aging, probably due to the deposition of organic matter at their surface during the treatment. Conversely, a net decrease of RMS roughness values was observed for experimental coatings. Excluding one sample (L23) which presented several impurities raising artificially its roughness, this phenomenon concerned all EC-0.6 and EC-1 samples probed in this work. It can then be hypothesized, that the surface of experimental coatings was kind of polished by the water flow although this effect was not obvious on topography images.

Thanks to their larger scale, SEM images allowed identifying other signs of aging. For example, they brought into light the contamination of the coatings during the aging process (Figs. S3 and S4, Supplementary content). Traces of organic matter could indeed be detected on most samples after aging, the highest concentrations being logically found for the runs where humic acids were present. As detailed in Supplementary content, some inorganic contamination was also regularly observed in the form of small oxides particles.

Apart from the contamination, the coatings seemed more or less able to maintain their integrity. No cracking of the photocatalytic layer was observed in the whole experiment and neither did it ripple. However some samples of experimental coatings exhibited a highly disturbed surface, as shown in Fig. 6a. Two striking new features appear on this image. First of all, some holes are present in the coating, leaving now visible the substrate whereas it was fully covered before aging. Secondly, several large and flat islands can be seen on top of the background layer, which although they resulted to be made of TiO_2 (EDX measurement, not shown), clearly differ from the initial agglomerates. These two features could be observed on several images corresponding to both EC batches but they were more frequent in NaCl and HA + NaCl runs (EC-1 samples). Besides, they seemed to be more numerous on samples that were irradiated with UVA, suggesting that both NaCl and UVA light may favor their appearance.

An insight on the formation of holes and TiO_2 flat islands can be gained through a detailed examination of the surface of experimental coatings after aging. First of all, the observation of partially removed TiO_2 agglomerates, like agglomerate 1 in Fig. 6c, led to the conclusion that holes were formed upon disappearance of TiO_2 agglomerates. Two mechanisms of removal could be evidenced. On the one hand, Fig. 6b indicated that some agglomerates may simply be swept by the water flow, while on the other hand, the blurry part of agglomerate 2 in Fig. 6c, suggested that a re-dispersion of the agglomerated TiO_2 nanoparticles may also take place. This second phenomenon could only be clearly stated on samples that were exposed to both NaCl and UVA. If we now consider the formation of TiO_2 flat islands, the feature that was identified as most relevant was the presence of dusty areas at the surface of aged experimental coatings, as highlighted in Fig. 6d. EDX analysis (not shown) revealed that this "dust" consisted in TiO_2 particles. Although the origin of these TiO_2 particles remains unclear, it can then be hypothesized that TiO_2 flat islands, such as that exampled in Fig. 6e, result from the diffusion of TiO_2 particles at the surface of the coating and their subsequent assembly into a more stable structure than the initial agglomerates. Interestingly, similar objects could be evidenced on Activ™ samples (Fig. 6f) in presence of NaCl and UVA light, although in a lower amount. These were besides the only signs of aging that could be detected on Pilkington Activ™ apart from the above-described contamination.

3.4. Loss of TiO_2

No difference was detected in sample weight before and after aging, suggesting there was no major loss of material. This could moreover be confirmed by thickness measurements on EC-0.6 and EC-1, as no lower values were found for aged samples than for their respective control (Table 3). Neither could any significant variations in the TiO_2 content of the coatings be evidenced by EDX. The efforts to assess TiO_2 emissions therefore focused on the elemental analysis of the water circulated in the flumes during the experiment.

Fig. 7 shows the concentration measured for TiO_2 in these waters as a function of water matrix and illumination. While the controls (not shown) exhibited concentrations below the detection limit of the equipment (0.16 μg L^{-1}), all the waters used

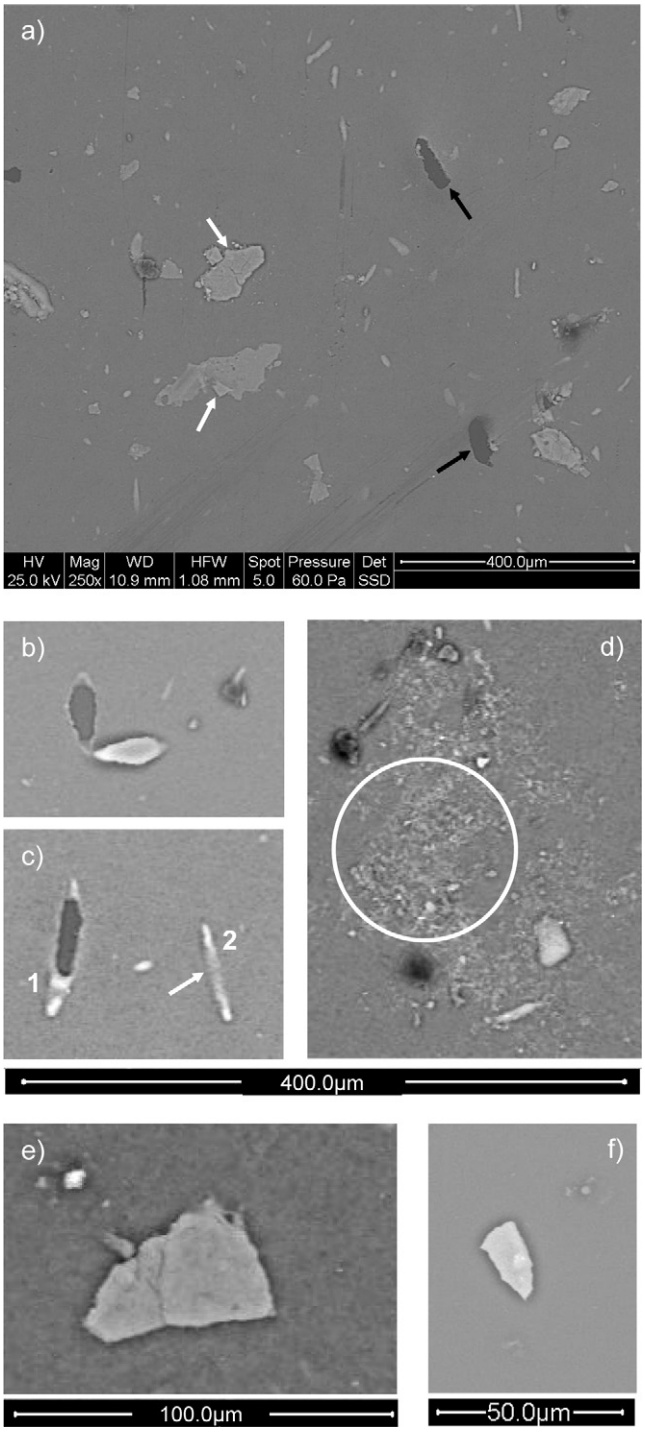

Fig. 6. Morphology of the coatings after aging. (a) SEM image of an EC-1 sample after 4 weeks of exposure to NaCl and UVA radiation. The dark arrows signal holes in the photocatalytic layer leaving the bare substrate visible. The white ones indicate newly formed TiO_2 islands. (b) SEM image of a TiO_2 agglomerate swept by the water flow and stripped off of its initial location. (c) SEM image of two disappearing TiO_2 agglomerates on an experimental coating. The white arrow signals disaggregating TiO_2 nanoparticles. (d) Mobile TiO_2 at the surface of experimental coatings. (e) Flat TiO_2 islands observed on EC-1 after 4 weeks of aging under HA + NaCl and UVA. (f) Flat TiO_2 islands observed on a Pilkington Activ™ sample after 4 weeks of aging under NaCl and UVA.

for aging contained titanium dioxide to a lower or higher extent. TiO_2 was then undeniably lost from both coatings under several circumstances. Moreover the composition of the water seemed to have a strong influence on TiO_2 emissions. Indeed, if DW and HA resulted in relatively low amounts of TiO_2 released over the 4 weeks of experiment, for both Pilkington Activ™ and EC-1 samples, emissions up to 5.9 $\mu g\,L^{-1}$ (Pilkington Activ™, Fig. 7b) and 104.5 $\mu g\,L^{-1}$ (EC-1 coatings, Fig. 7a) were recorded in presence of NaCl. Although this enhanced release could be ascribed to the lower mechanical properties of EC-1 or to the higher photocatalyst load of these samples for experimental coating, the parallel increase of TiO_2 losses in Pilkington Activ™ under the same conditions establishes irrefutably the influences of sodium chloride on emissions. Besides, this effect was magnified when humic acids were added to NaCl, reaching the highest TiO_2 levels of the whole experiment: 30.8 $\mu g\,L^{-1}$ and 150.5 $\mu g\,L^{-1}$ for Pilkington Activ™ and EC-1 samples, respectively. At the other extreme, the lowest TiO_2 losses were observed for HA runs on experimental coatings and DW runs on Pilkington Activ™. In most cases, the samples irradiated with UV-light released higher amounts of TiO_2 than the samples aged under the same condition in darkness.

Although both coatings displayed similar tendencies of release, the magnitude of their emissions differed and the loss of TiO_2 was generally higher on experimental coatings than on Pilkington Activ™. One should however put this result in perspective with the much lower initial TiO_2 content of Pilkington Activ™. Taking into account the exposed surface (10 samples, i.e. $7.5 \times 10^{-3}\,m^2$), the cumulative release of TiO_2 from the two coatings during the 4 weeks of experiment is given in Table 4. It is interesting to see that on average, these values lay in the same range that experimental data obtained by Kaegi et al. [28] from runoff water of fresh paints after rain events. Yet they generally remained lower, consistently with the fact that paints have a very high TiO_2 content and that efforts are made in photocatalytic coatings to achieve a better immobilization of TiO_2 nanoparticles. The *ca.* 10 $mg\,m^{-2}$ of Ti emissions (equivalent to 16.7 $mg\,m^{-2}$ TiO_2) accumulated over one month in Kaegi's study are only overcome on experimental coatings aged under the most aggressive conditions: HA + NaCl and UVA.

In outdoor air applications (self-cleaning surfaces, air purification) the values calculated here would probably represents a worst case scenario, as a continuous water flow seems exaggerated with respect to occasional rain events. On the contrary in water treatment application, high water flows are likely, and our values may actually underestimate real releases. Whatever the case, they have to be put in perspective with the fact that they correspond to relatively fresh materials. Loosely bound particles probably account for a great part in the observed releases and TiO_2 emissions could decrease after the first weeks of use, as reported before for paints [28]. Further investigations are then needed to evaluate the distribution of TiO_2 emissions over time.

4. Discussion

A better understanding of aging mechanisms and their consequences can be gained through the comparative analysis of the results. For instance, it is interesting to note that the loss of TiO_2 is at the same time not high enough, and too dependent on the aging conditions, to explain the almost systematic decrease in photocatalytic activity observed for Pilkington Activ™ and experimental coatings. Some deactivation of the photocatalyst must take place

Table 4
Cumulative release of TiO_2 over 4 weeks, expressed in $mg\,m^{-2}$.

Water typology	Experimental coatings		Pilkington Activ™	
	Dark	UVA	Dark	UVA
DW	0.73	1.72	0.06	0.12
HA	0.12	0.09	0.10	0.27
NaCl	3.60	13.93	0.79	0.24
HA + NaCl	10.50	20.07	2.49	4.11

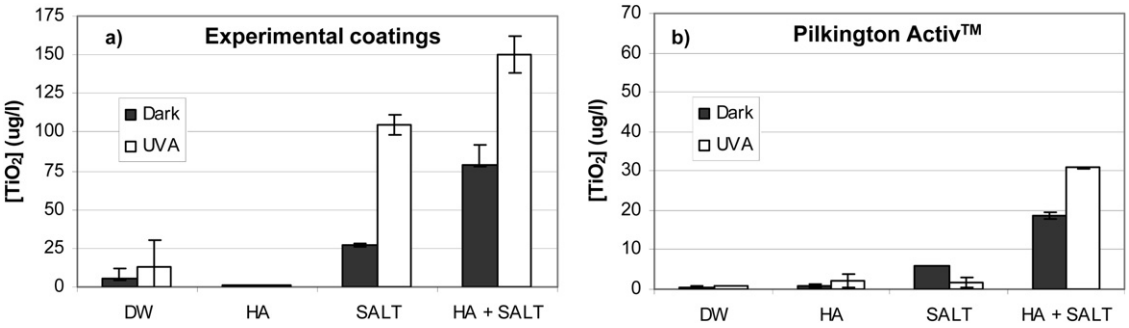

Fig. 7. Emissions of TiO_2. Concentration of aging waters in TiO_2 as measured by ICP-OES for (a) experimental coatings and (b) Pilkington Activ™.

which cannot be ascribed to changes in TiO_2 crystalline phase (very unlikely in our experimental conditions).

The inhibitory action of both organic and inorganic substances presents in real waters, on the photocatalytic reaction has been pointed out repeatedly [44,45]. Humic acids are have been cited several times as a major retarding agent [46–48] and chloride ions are known to reduce degradation efficiencies at pH below TiO_2 isoelectric point [49–51]. In our experiments the loss of photocatalytic activity is very similar in HA, NaCl and HA + NaCl runs and their specific influence does not appear clearly. Furthermore deactivation was also observed on samples exposed solely to deionized water. Other compounds must then be at stake.

It is important to highlight that in contrast with previous works, deactivation occurs here upon simulated aging, before photocatalytic oxidation experiments. It proved moreover to be quite persistent, a 24 h exposure to UVA radiation (in air) being insufficient to regenerate the materials. Under such circumstance an inhibition of the photocatalytic reaction by radical scavenging does not appear plausible. Blockage of the active sites of the photocatalyst is more likely.

We observed that in spite of the initial purity of the water used, some contamination was deposited at the surface of the coatings (Figs. S3 and S4, Supplementary content), which may partly obstruct TiO_2 reactive sites. Besides, aging experiments were carried out in flumes open to the atmosphere and absorption of ambient CO_2 by water will then take place over time. This will lead to the formation of carbonate species in water, which can also be detrimental to photocatalytic activity [52,53]. Guillard et al. [54] suggested that in addition to radical scavenging and competitive adsorption (not relevant for methylene blue), these compounds could form an inorganic salt layer at the surface of the photocatalyst. No such layer could be evidenced on SEM-EDX analysis. Nevertheless, final water pH measured in the flumes is consistent with CO_2 absorption (Fig. S2, Supplementary content) and the formation of an inorganic layer would explain the persistence of the deactivation phenomenon described in this work.

Interestingly the extent of deactivation differed between the two types of coatings tested. While Pilkington Activ™ lost in average 65% of its photocatalytic activity after 4 weeks of aging, experimental coatings were proven to maintain it at 80%. This suggests that the formulation of the photocatalytic coatings can be tuned to enhance their resistance to deactivation.

Unlike photocatalytic activity, the degradation of mechanical properties related well with TiO_2 emissions, at least for experimental coatings. On these samples, the highest emissions corresponded to the strongest mechanical damage, while a good maintaining of the mechanical properties of EC-0.6 in HA runs gave the lowest TiO_2 levels of the whole experiment. Based on the opposite effect of UV-light on adhesion and hardness, a mechanism for the release of the photocatalytic material can be proposed. Indeed, if UV-light was found to enhance the degradation of film hardness, it seemed to attenuate the loss of adhesion. This is contradictory with the increased TiO_2 emissions observed under the same conditions and suggests therefore that TiO_2 losses do not result from a detachment of the whole coating. Instead, the reduction in film hardness hints to some change in EC matrix finally leading to the release of TiO_2. This hypothesis seems to be confirmed by SEM images, where the only holes present in aged coatings are due to the removal of TiO_2 agglomerates and no detachment of the matrix is witnessed.

SEM images also indicated that at least two mechanisms may be involved in TiO_2 emissions. On the one hand, some TiO_2 agglomerates are stripped off of the coatings by the water flow, this phenomenon being probably promoted in NaCl and HA + NaCl runs by the weakening of matrix hardness. On the other hand an interesting phenomenon of dispersion of TiO_2 agglomerates in presence of NaCl and UV-light was also evidenced. Given the changes observed in the mechanical properties of experimental coatings, a third phenomenon is proposed, being the direct liberation of TiO_2 nanoparticles from the siliceous matrix, as a consequence of its loosening. Noteworthy is that while the first mechanism will lead to the emission of big TiO_2 agglomerates, both the dispersion of TiO_2 agglomerates and the liberation of TiO_2 nanoparticles from the siliceous matrix will result in the presence of suspended TiO_2 nanoparticles (or small agglomerates) in the aging water. They may also be at the origin of the TiO_2 "dust" observed on some samples, which was identified as a precursor to the formation of flat TiO_2 islands.

TiO_2 flat islands could also be observed on Pilkington Activ™. Furthermore both materials followed almost identical emission profiles and were found to respond to environmental conditions in the same way. Common mechanisms of emission may then be at stake in the two coatings, which are influenced by the presence of NaCl, HA and UVA but independent from the siliceous matrix of experimental coatings. They must therefore rely on specific interactions between TiO_2, the glass substrate, NaCl, HA and UVA, and as such, could take place on many different photocatalytic coatings. If the enhanced TiO_2 emissions in presence of HA can easily be explained by the stabilization these compounds generally induce for suspended TiO_2 nanoparticles [55–58], elucidating the influence of NaCl and UVA light is more delicate. SEM observations suggest that it could be related to the dispersion of TiO_2 particles or their detachment from the glass substrate. We can then make the hypothesis that sodium chloride and ultraviolet light modify somehow TiO_2–TiO_2 and TiO_2–glass substrate interaction, entailing the release of TiO_2 nanoparticles in the water. Earlier reports already proposed that high concentrations of salt could have such an effect on TiO_2 [59,60] and other materials [61,62]. The possible influence of UVA on these phenomena is however new.

Finally, it has to be highlighted that among all investigated techniques, only ICP-OES was able to detect TiO_2 emissions. Weighing, thickness measurements and estimations of TiO_2 content by EDX did not show enough sensitivity, while indirect indicators such as photocatalytic activity were twisted by interfering deactivation

phenomena. The best correlation with TiO_2 emissions was found for mechanical testing. However some limitations are evidenced for these measurements on Pilkington Activ™, which displayed unaltered mechanical properties and still showed TiO_2 emissions. The applicability of mechanical properties as an indicator for TiO_2 emissions then cannot be granted under all circumstances and ICP-OES remains the only reliable way to detect TiO_2 release at these levels.

5. Conclusion

The aging of photocatalytic coatings under a water flow was investigated in terms of loss of photocatalytic properties, mechanical damages and TiO_2 nanoparticles release, for two very different materials. In spite of their different nature and properties, some common features arise from the aging of these coatings, which may also be of relevance for other photocatalytic coatings. For instance this work highlights a deactivation of the active sites of TiO_2 upon prolonged immersion in water, which may reduce the performance of photocatalytic materials. Moreover, for both type of coatings, a release of TiO_2 nanoparticles was found, suggesting that the use of photocatalytic coatings with surface-bound nanoparticles does not completely avoid the entry of nanomaterials into the environment.

Strongest releases were measured in the presence of NaCl, humic acids and under UVA illumination. In a more general way, environmental parameters were found to cause most of the described phenomena, while the intrinsic properties of the photocatalytic coatings (chemical composition, thickness) mainly had an influence on their magnitude. The major difference observed between the two coatings was in their ability to maintain good mechanical properties. While experimental coatings experienced severe damages, Pilkington Activ™ seemed to be unaffected by water attrition, even if this did not preserve it from deactivation or avoided the release of TiO_2 nanoparticles. This shows that a multiplicity of effects can result from the aging of photocatalytic coatings that are not necessarily reflected in their macroscopic properties (aspect, weight, mechanical properties, etc.). Comprehensive assessments of aging, such as that presented in this work, are therefore needed to improve our knowledge on the long run performance of photocatalytic coatings and their environmental impact. Besides, this would enable an early detection of the release of TiO_2 nanoparticles to the environment and open the possibility to minimize it through the development of safer products binding the photocatalyst more firmly to its substrate.

Acknowledgments

This work was jointly funded by Cantabria Government in the framework of the AquaNAN project and TECNALIA Foundation under its internal Nanotechnology Programme. Great thanks are due to Txomin Laburu for his determining help in the design and elaboration of the aging flumes and Carmen del Río for ICP-OES measurements.

Appendix A. Supplementary data

Supplementary data associated with this article can be found, in the online version, at http://dx.doi.org/10.1016/j.apcatb.2012.04.027.

References

[1] S. Wang, H.M. Ang, M.O. Tade, Environment International 33 (2007) 694.
[2] K. Rajeshwar, M.E. Osugi, W. Chanmanee, C.R. Chenthamarakshan, M.V.B. Zanoni, P. Kajitvichyanukul, R. Krishnan-Ayer, Journal of Photochemistry and Photobiology C 9 (2008) 171.
[3] S. Ahmed, M.G. Rasul, R. Brown, M.A. Hashib, Journal of Environmental Management 92 (2011) 311.
[4] K. Kabra, R. Chaudhary, R.L. Sawhney, Environmental Progress 27 (2008) 487.
[5] J. Sá, C.A. Agüera, S. Gross, J.A. Anderson, Applied Catalysis B 85 (2009) 192.
[6] R.-A. Doong, T.-C. Hsieh, C.-P. Huang, Science of the Total Environment 408 (2010) 3334.
[7] H. Jang, S. Kim, S. Kim, Journal of Nanoparticle Research 3 (2001) 141.
[8] W. Hao, S. Zheng, C. Wang, Journal of Materials Science Letters 21 (2002) 1627.
[9] H. Lin, C.P. Huang, W. Li, C. Ni, S.I. Shah, Y.-H. Tseng, Applied Catalysis B 68 (2006) 1.
[10] M. Anpo, T. Shima, S. Kodama, Y. Kubokawa, Journal of Physical Chemistry A 91 (1987) 4305.
[11] Z. Zhang, C. Wang, R. Zakaria, J. Ying, Journal of Physical Chemistry B 102 (1998) 10871.
[12] A. Maira, K. Yeung, C. Lee, P. Yue, C. Chan, Journal of Catalysis 192 (2000) 185.
[13] C. Almquist, P. Biswas, Journal of Catalysis 212 (2002) 145.
[14] M. Toyoda, Y. Nanbu, Y. Nakazawa, M. Hirano, M. Inagaki, Applied Catalysis B 49 (2004) 227.
[15] S. Liu, N. Jaffrezic, C. Guillard, Applied Surface Science 255 (2008) 2704.
[16] H.-W. Chen, S.-F. Su, C.-T. Chien, W.-H. Lin, S.-L. Yu, C.-C. Chou, J.J.W. Chen, P.-C. Yang, FASEB Journal 20 (2006) 2393.
[17] D.B. Warheit, T.R. Webb, K.L. Reed, S. Frerichs, C.M. Sayes, Toxicology 230 (2007) 90.
[18] K. Inoue, H. Takano, M. Ohnuki, R. Yanagisawa, M. Sakurai, A. Shimada, K. Mizushima, T. Yoshikawa, International Journal of Immunopathology and Pharmacology 21 (2008) 197.
[19] G. Federici, B.J. Shaw, R.D. Handy, Aquatic Toxicology 84 (2007) 415.
[20] C.S. Ramsden, T.J. Smith, B.J. Shaw, R.D. Handy, Ecotoxicology 18 (2009) 939.
[21] V. Aruoja, H.-C. Dubourguier, K. Kasemets, A. Kahru, Science of the Total Environment 407 (2009) 1461.
[22] N.B. Hartmann, F. Von der Kammer, T. Hofmann, M. Baalousha, S. Ottofuelling, A. Baun, Toxicology 269 (2010) 190.
[23] M. Keshmiri, M. Mohseni, T. Troczynski, Applied Catalysis B 53 (2004) 209.
[24] M. Bizarro, M.A. Tapia-Rodríguez, M.L. Ojeda, J.C. Alonso, A. Ortiz, Applied Surface Science 255 (2009) 6274.
[25] L. Reijnders, Journal of Hazardous Materials 152 (2008) 440.
[26] L. Reijnders, Polymer Degradation and Stability 94 (2009) 873.
[27] R. Kaegi, A. Ulrich, B. Sinnet, R. Vonbank, A. Wichser, S. Zuleeg, H. Simmler, S. Brunner, H. Vonmont, M. Burkhardt, M. Boller, Environmental Pollution 156 (2008) 233.
[28] R. Kaegi, B. Sinnet, S. Zuleeg, H. Hagendorfer, E. Mueller, R. Vonbank, M. Boller, M. Burkhardt, Environmental Pollution 158 (2010) 2900.
[29] L.-Y. Hsu, H.-M. Chein, Journal of Nanoparticle Research 9 (2007) 157.
[30] L. Zhang, P. Zhang, S. Chen, Chinese Journal of Catalysis 28 (2007) 299.
[31] N. Yao, K. Lun Yeung, Chemical Engineering Journal 167 (2011) 13.
[32] Y. Chen, D.D. Dionysiou, Applied Catalysis B 62 (2006) 255.
[33] A. Mills, A. Lepre, N. Elliott, S. Bhopal, I.P. Parkin, S.A. O'Neill, Journal of Photochemistry and Photobiology A 160 (2003) 213–224.
[34] P. Chin, D.F. Ollis, Catalysis Today 123 (2007) 177–188.
[35] I. Horcas, R. Fernaĭndez, J.M. Goĭmez-Rodriĭguez, J. Colchero, J. Goĭmez-Herrero, A.M. Baro, Review of Scientific Instruments 78 (2007) 013705.
[36] M. Langlet, A. Kim, M. Audier, C. Guillard, J. Herrmann, Thin Solid Films 429 (2003) 13.
[37] G. Balasubramanian, D.D. Dionysiou, M.T. Suidan, I. Baudin, J.-M. Laı□né, Applied Catalysis B 47 (2004) 73.
[38] Y. Chen, D.D. Dionysiou, Applied Catalysis B 69 (2006) 24.
[39] M.C. Hidalgo, D. Bahnemann, Applied Catalysis B 61 (2005) 259.
[40] G. Bolelli, V. Cannillo, R. Gadow, A. Killinger, L. Lusvarghi, J. Rauch, Surface and Coatings Technology 203 (2009) 1722.
[41] F. Bondioli, R. Taurino, A.M. Ferrari, Journal of Colloid and Interface Science 334 (2009) 195.
[42] K. Murugan, T.N. Rao, G.V.N. Rao, A.S. Gandhi, B.S. Murty, Materials Chemistry and Physics 129 (2011) 810.
[43] A.C. Fischer-Cripps, Surface and Coatings Technology 200 (2006) 4153.
[44] A. Rincon, Applied Catalysis B 51 (2004) 283.
[45] J. Chen, Z. Hu, D. Wang, C. Gao, R. Ji, Applied Catalysis B 258 (2010) 28.
[46] E. Selli, D. Baglio, L. Montanarella, G. Bidoglio, Water Research 33 (1999) 1827.
[47] C. Lin, K. Lin, Chemosphere 66 (2007) 1872.
[48] W.A. Adams, C.A. Impellitteri, Journal of Photochemistry and Photobiology A 202 (2009) 28.
[49] H.Y. Chen, O. Zahraa, M. Bouchy, Journal of Photochemistry and Photobiology A 108 (1997) 37.
[50] A. Piscopo, D. Robert, J.V. Weber, Applied Catalysis B 35 (2001) 117.
[51] K. Selvam, M. Muruganandham, I. Muthuvel, M. Swaminathan, Chemical Engineering Journal 128 (2007) 51.
[52] A. Lair, C. Ferronato, J.-M. Chovelon, J.-M. Herrmann, Journal of Photochemistry and Photobiology A 193 (2008) 193.
[53] M. Pelaez, A.A. de la Cruz, K. O'Shea, P. Falaras, D.D. Dionysiou, Water Research 45 (2011) 3787.
[54] C. Guillard, E. Puzenat, H. Lachheb, A. Houas, J.-M. Herrmann, International Journal of Photoenergy 7 (2005) 1.
[55] B.J.R. Thio, D. Zhou, A.A. Keller, Journal of Hazardous Materials 189 (2011) 556.
[56] F. von der Kammer, S. Ottofuelling, T. Hofmann, Environmental Pollution 158 (2010) 3472.
[57] R.F. Domingos, N. Tufenkji, K.J. Wilkinson, Environmental Science & Technology 43 (2009) 1282.

[58] Y. Zhang, Y. Chen, P. Westerhoff, J. Crittenden, Water Research 43 (2009) 4249.
[59] F. Mange, P. Couchot, A. Foissy, A. Pierre, Journal of Colloid and Interface Science 159 (1993) 58.
[60] H. Yotsumoto, R.-H. Yoon, Journal of Colloid and Interface Science 157 (1993) 426.
[61] N. Kallay, B. Biškup, M. Tomić, E. Matijević, Journal of Colloid and Interface Science 114 (1986) 357.
[62] J.A. Molina-Bolıívar, F. Galisteo-González, R. Hidalgo-Alvarez, Colloids and Surfaces B 14 (1999) 3.
[63] CRC Handbook of Chemistry and Physics, 69th ed., CRC Press, Boca Raton, FL, 1988.
[64] T. Bleninger, A. Niepelt, G.H. Jirka, Seawater Density and Viscosity Calculator, 2009.